



A new approach for the synthesis of new benzothiazole derivatives and their biological and docking evaluation

Mina Nader^a, Ehab Abdel-Latif^a, Ahmed A. Fadda^{a*}, Yasmin Tag^b, Nanees N. Soliman^a

^aDepartment of Chemistry, Faculty of Science, Mansoura University, Egypt

^bOral Biology Department, Faculty of Oral and Dental Medicine, Delta University for Science and Technology, Mansoura, Egypt

* Corresponding Author: afadda50@yahoo.com

Received: 23/7/2023
Accepted: 21/9/2023

Abstract: Here, we describe how hydrazoneyl malononitrile compound **2** reacts with a variety of secondary amines in boiling ethanol to synthesis the corresponding acrylonitrile compounds **3–8**. Additionally, compound **2** produced the pyrazole derivative **9** and the pyridazine derivative **11**, respectively, through reactions with hydrazine hydrate and malononitrile. Additionally, in a boiling solution of ethanolic sodium ethoxide, malononitrile and **7** reacted to form pyrimidine **14**. *N*-Acetylpentaacetate **15** was produced by heating **7** in boiling acetic anhydride, and *N*-acetyl-2-pyridone **16** was formed by prolonged heating in DMF with catalytic amounts of TEA. In addition, when compound **7** and triethyl orthoformate were reacted with "acetic anhydride", the resulting "ethoxymethyleneamino" **17** was produced. By refluxing a solution of compound **7** and DMF/DMA in dry xylene, dimethyl formimidamide **18** was produced. The phthalimide derivatives **19–26** were formed by refluxing acid anhydride derivatives with compound **7** in DMF and acetic acid. Compounds **7** and **8** have been determined to have the strongest antioxidant activity. The effectiveness of the newly synthesized compounds **3, 4, 7, 8, 9, 11, 14–18, and 19–26** was evaluated for their antitumor activities against four cell lines; HepG2, WI-38, VERO, and MCF-7. Additionally, it was found that the two drugs, **14**, and **20**, exhibit potent efficacy against the four cell lines tested. Molecular docking (PDB=1M17) was used to examine the binding disposition of the docked compounds, in particular **7, 8, 11, and 14**, towards the binding site of the EGFR complexed with the co-crystallized ligand.

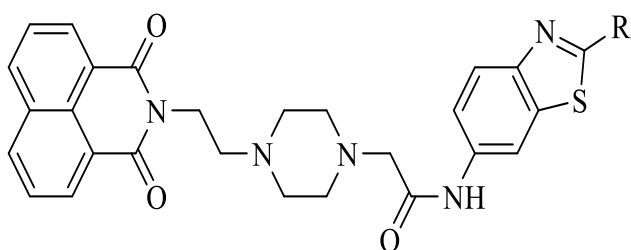
keywords: Enaminonitrile; Pyrazole; Pyrimidine; Pyridine; Malononitrile; N-methyl glucamine

1. Introduction

One of the serious disorders where abnormal cells spread and divide uncontrollably without any control is cancer. Cancer is linked to genetic changes; specifically, it affects the manner in which genes are expressed and causes abnormal gene activity [1, 2]. According to a recent WHO estimate, cancer was one of the main causes of death for almost 10 million people worldwide in 2018. Heterocyclic compounds have been essential for the creation of new and effective anticancer drugs in medicinal chemistry. Among the benzene-fused heterocyclic compounds, benzothiazole is one of the heterocyclic scaffolds that is recognized as a potent cytotoxic agent. One of the

pharmacologically preferred rings is benzothiazole, which exhibits substantial anticancer activity in addition to "anti-inflammatory", [3, 4] "antifungal", [5, 6] "antiviral", [7, 8] "analgesic", [9, 10] "antioxidant", [8, 9] "antipsychotic", [10, 11] "anticonvulsant", [12, 13] and "antidiabetic activity". Anticancer chemotherapy contains a number of unfavorable side effects, including selectivity, adverse events, multiple drug resistance, and undesirable side effects, in addition to the different activities of benzothiazole. To overcome these obstacles, it is essential to create powerful, safe, and effective benzothiazole scaffolds that include

cytotoxic agents. However, due to their strong cytotoxic effect *in vivo* and *in vitro* models, amino benzothiazole, aryl benzothiazole, and structural hybrids of benzothiazole have gained significant interest in the quest for chemotherapeutic drugs. According to Rao et al. [14], compounds (A) and (B) are naphthalimide-benzothiazole derivatives that effectively block topoisomerase II by intercalating with DNA. Furthermore, derivatives (A) and (B) both exhibited strong anticancer activity; future research could lead to the development of strong inhibitors that target topoisomerase.

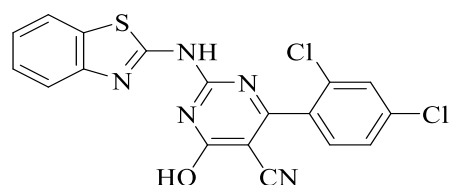


A, R= H
B, R= CH₃

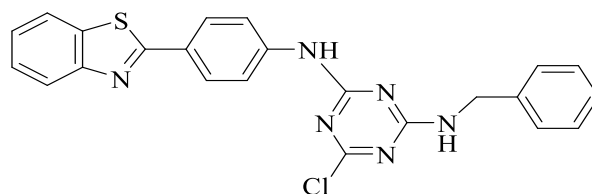
Figure 1: Examples of benzothiazole-based on topoisomerase inhibitors

Compound (C) is a powerful tyrosine kinase inhibitor, according to Chikhale et al. [15]. 2-aminobenzoyl derivative of compound (C) that contains pyrimidines demonstrated strong cytotoxicity against the human cancer cell lines HEK293T and WRL68.

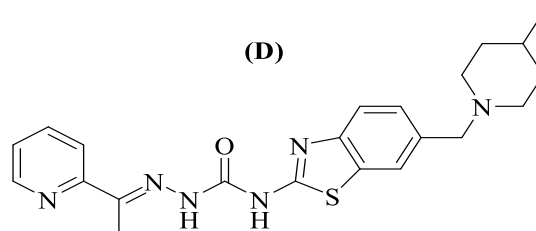
Novel triazine-bearing compounds have been described by Kumar et al. [16] as effective anticancer drugs. The majority of the substances were discovered to be effective against specific cancer cell lines, including PC3, HT29, MCF7, and DU145. The compound (D) in the series featured a chloro substituent at position C3 of the triazine ring, which gave it a minor amount of activity against the selected cell lines. Tri-substituted triazine derivatives, as opposed to di-substituted derivatives, appear to be more potent, according to the SAR of the compounds. Benzothiazole derivatives (E) were found to activate apoptosis in U937 cells in a dose-dependent manner, according to Junjie et al. [17]. Additionally, research on compound E's caspase-3 activation showed that it had a powerful activation activity (99 %).



(C)



(D)



(E)

Figure 2: Benzothiazole-containing compounds as anticancer agents

Most azo dye compounds exhibit a variety of biological activities, including azo reduction, monoamine oxidase inhibition, mutagenicity, carcinogenesis, as well as additional uses in both medicine and industry [18, 19]. Enaminonitriles play an important role as intermediates in the synthesis of various heterocyclic compounds exhibiting a wide range of biological properties

[20-26]. Numerous heterocyclic compounds exhibit significant pharmacological applications, including anti-inflammatory [27], antitumor [28, 29], antibacterial and antifungal activity [30], and used as analgesic agents [31]. These compounds can be synthesized by reacting the amino and cyano groups within them with commonly used reagents. The biological effects of sugar and its associated molecules, including their anticancer, antiviral, and antibiotic properties, are well documented [32, 33]. Consequently, we explored the synthesis of novel heterocyclic compounds incorporating glucaminoid moieties. This approach aimed to enhance the biological activity achieved through linking sugar units with diverse heterocyclic rings.

2. Results and Discussion

2.1. Chemistry

The significant key of this study, *N*-(benzothiazol-2-yl)carbonohydrizonoyl dicyanide (**2**) was produced through the reaction between diazotized 2-aminobenzothiazole (**1**) and malononitrile. The acrylonitriles **3-8** were synthesized by reacting compound **2** with various secondary amines in refluxing ethanol, including piperidine, morpholine, piperazine, diphenylamine, *N*-methylglucamine, and/or diethanolamine (**Scheme 1**).

Based on the data of elemental and spectral analyses, the structures of the enaminonitrile derivatives **3-8** were identified. In addition to the other predicted bands, the IR spectra of the derivatives **3-8** generally displayed characteristic bands within $= 3450-3350\text{ cm}^{-1}$ due to the NH_2 group and bands within $= 2220-2180\text{ cm}^{-1}$ relating to the CN group. The $^1\text{H-NMR}$ of compound **3** showed the piperidine ring's 3CH_2 multiplets at $\delta 1.55-1.70$ and $1.72-1.85$ ppm, the piperidine moiety's $\text{CH}_2\text{-N-CH}_2$ triplet sharp signal at $\delta 3.06$ ppm, one signal at $\delta 6.51$ ppm corresponding to NH_2 protons, and multiple signals at $\delta 6.51$ ppm. Furthermore, to $\text{CH}_2\text{-O-CH}_2$ protons, while in compound **4** the $^1\text{H-NMR}$ displayed two triplet signals at $\delta 3.14$ and $\delta 3.67$ ppm according to $-\text{N-}[\text{CH}_2]_2$ the methylene protons, respectively. While compound **5**'s $^1\text{H-NMR}$ results showed two triplets at $\delta 3.16$ and 3.69 ppm, respectively that were associated with $-\text{N-}[\text{CH}_2]_2$ and $-\text{N-}[\text{CH}_2]_2$. A singlet for the OH proton was found at $\delta 3.93$ ppm, multiplets for 4OH groups were found at $\delta 4.35-4.51$ ppm, and multiplets for four CH and two CH_2 were found at $\delta 3.53$ ppm in the $^1\text{H-NMR}$ of **7**. Indicated two doublet signals at $\delta 7.25$ and 7.53 ppm from four aromatic protons as well as one signal from N-CH_3 protons at $\delta 3.04$ ppm. The $^1\text{H-NMR}$ spectrum for compound **8** showed two triplet signals at $\delta 3.16$ and 3.87 ppm, respectively, to identify the protons of $-\text{N-}[\text{CH}_2]_2$ and 2 O-CH_2 groups. Additionally, it showed two signals, one each from 2 OH and NH_2 protons, at $\delta 4.85$ and 6.50 ppm.

The reaction of hydrazoneyl malononitrile compound **2** with the hydrazine hydrate (**Scheme 1**) led to the discovery of diamino-

pyrazole analogue **9**. Additionally, it was discovered that compound **2** served as a crucial step in the synthesis of an intriguing pyridazine derivative. In an ethanolic solution, malononitrile and compound **2** interacted, and the reaction was catalyzed by sodium ethoxide. Through compound **10**, which was synthesized by linking the CN group of compound **2** with the CH_2 group of malononitrile, followed by a cycloaddition reaction, the result was the pyridazine derivative **11** (**Scheme 1**).

The $^1\text{H-NMR}$ spectrum of compound **9** displayed the aromatic protons at $\delta 7.41$ and 7.70 ppm, as well as two exchangeable singlet signals at $\delta 6.20$ and 12.53 ppm that were attributed to 2NH_2 and NH protons, respectively. Based on its accurate spectroscopic data, Structure **11** was confirmed. The IR spectrum of **11** identified absorptions at $3450-3336$, and 3214 cm^{-1} according to the NH_2 and N-H moieties. M^+ was displayed in the MS spectrum at m/z (%) = 293 (M^+ , 48) corresponding to the formula $\text{C}_{13}\text{H}_7\text{N}_7\text{S}$.

Additionally, in a boiling solution of ethanolic sodium ethoxide, malononitrile and compound **7** reacted to form pyrimidine **14**. Spectroscopic analysis was used to infer structure **14**. N-CH_3 , OH, and NH_2 protons all had singlets in the $^1\text{H-NMR}$ at $\delta 3.04$, 3.93 , and 8.45 ppm, respectively. The M^+ in the MS spectrum could be found at m/z (%) = 488 (M^+ , 40). (**Scheme 2**).

Compound **15** was obtained by heating **7** with acetic anhydride in boiling pyridine (**Scheme 3**). The structure of compound **15** was determined based on the spectroscopic investigation. The lack of an amino group was revealed in the IR spectrum. The $^1\text{H-NMR}$ revealed a singlet at $\delta 2.29$ ppm due to 2 N-COCH_3 protons, and a multiplet signal at $\delta 2.03$ ppm according to 5 OCOCH_3 protons. The M^+ at m/z (%) = 716 (M^+ , 46) in the MS spectrum was identified as belonging to the compound $\text{C}_{31}\text{H}_{36}\text{N}_6\text{O}_{12}\text{S}$.

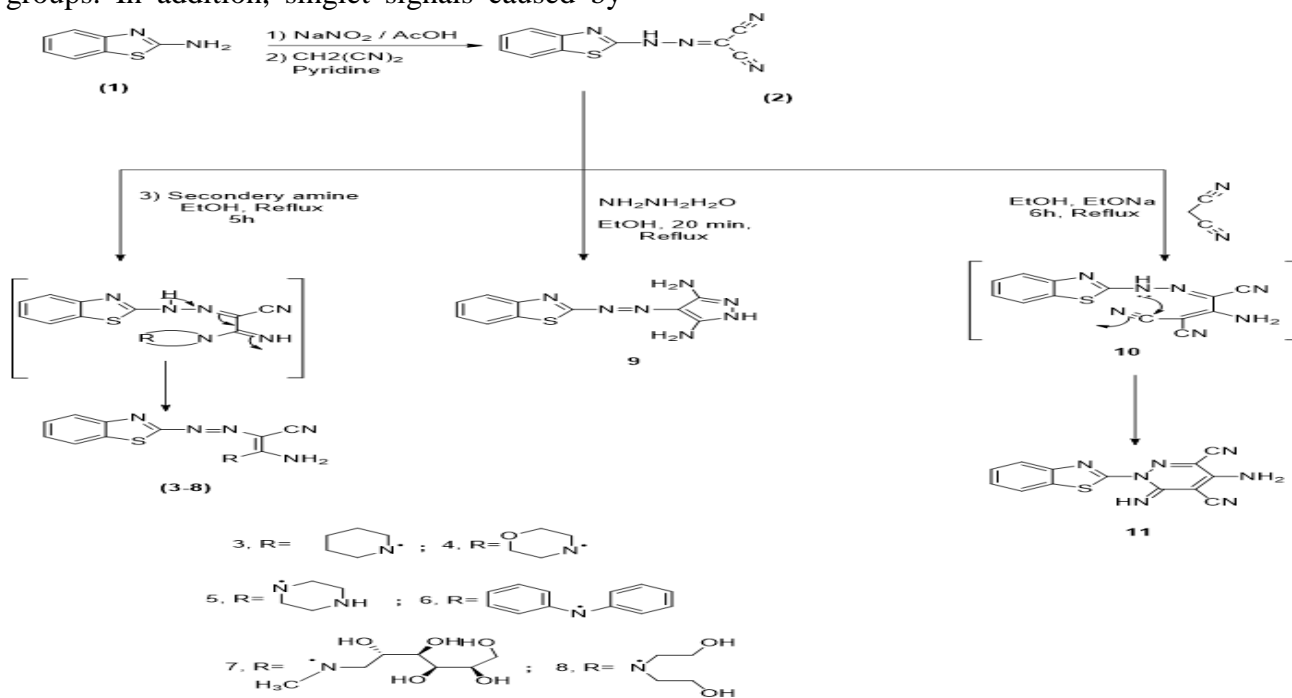
When compound **15** is cyclized, the equivalent pyridine derivative **16** is formed when heated for an extended period of time in refluxing DMF and triethylamine (**Scheme 3**).

Moreover, when compound **7** and triethyl orthoformate were reacted in acetic anhydride, ethoxymethyl eneamino derivative **17** was

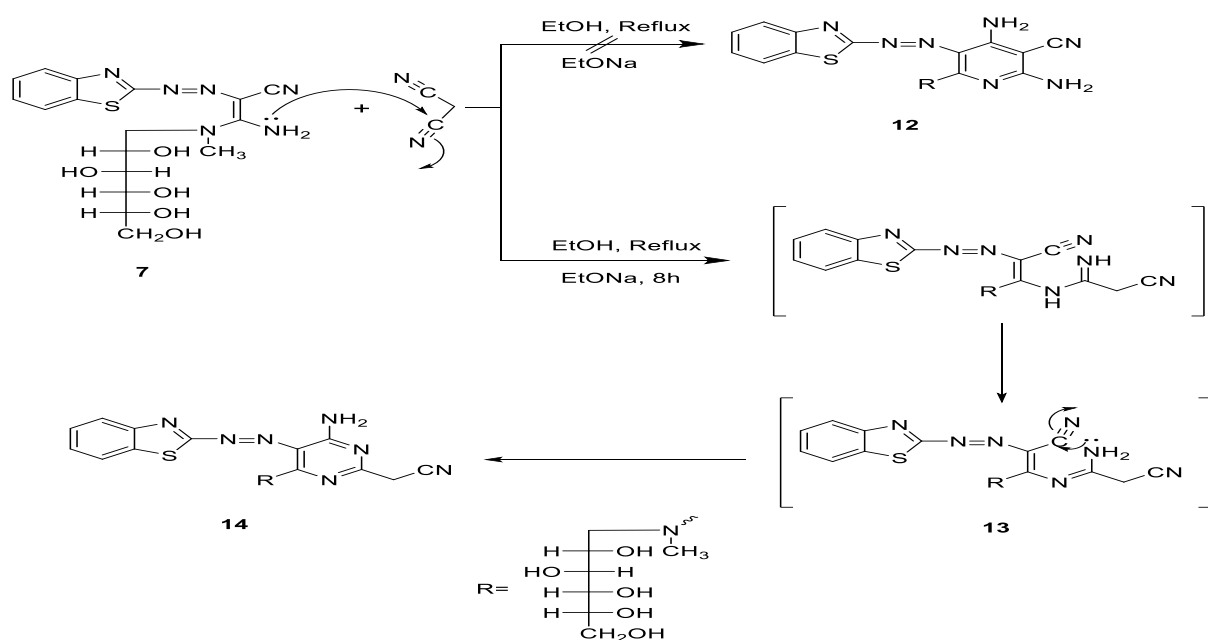
formed. Additionally, it was found that heating **7** with DMF/DMA in anhydrous xylene results in the synthesis of compound **18** (Scheme 3).

By spectroscopic investigation, the structures of compounds **17** and **18** were clarified. Compounds **17** and **18** each had distinctive bands in their IR spectra at 2179 and 2177 cm^{-1} , which can be attributed to CN groups. In addition, singlet signals caused by

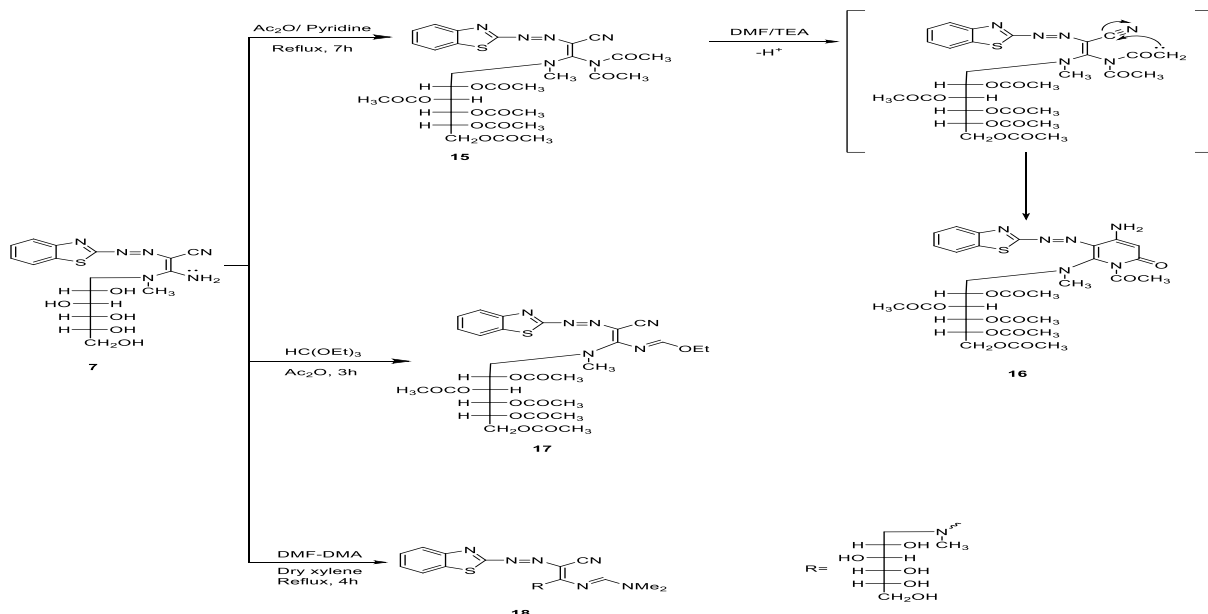
the CH=N proton appeared at δ 8.50 and 8.73 ppm in the $^1\text{H-NMR}$ spectrum of derivatives **17** and **18**, respectively. Moreover, the molecular ion peaks of **17** and **18** were found in the MS at m/z (%) = 688 (M^+ , 44) and 477 (M^+ , 38), respectively, and were assigned to the molecules $\text{C}_{30}\text{H}_{36}\text{N}_6\text{O}_{11}\text{S}$ and $\text{C}_{20}\text{H}_{27}\text{N}_7\text{O}_5\text{S}$, respectively (Scheme 3).



Scheme 1



Scheme 2

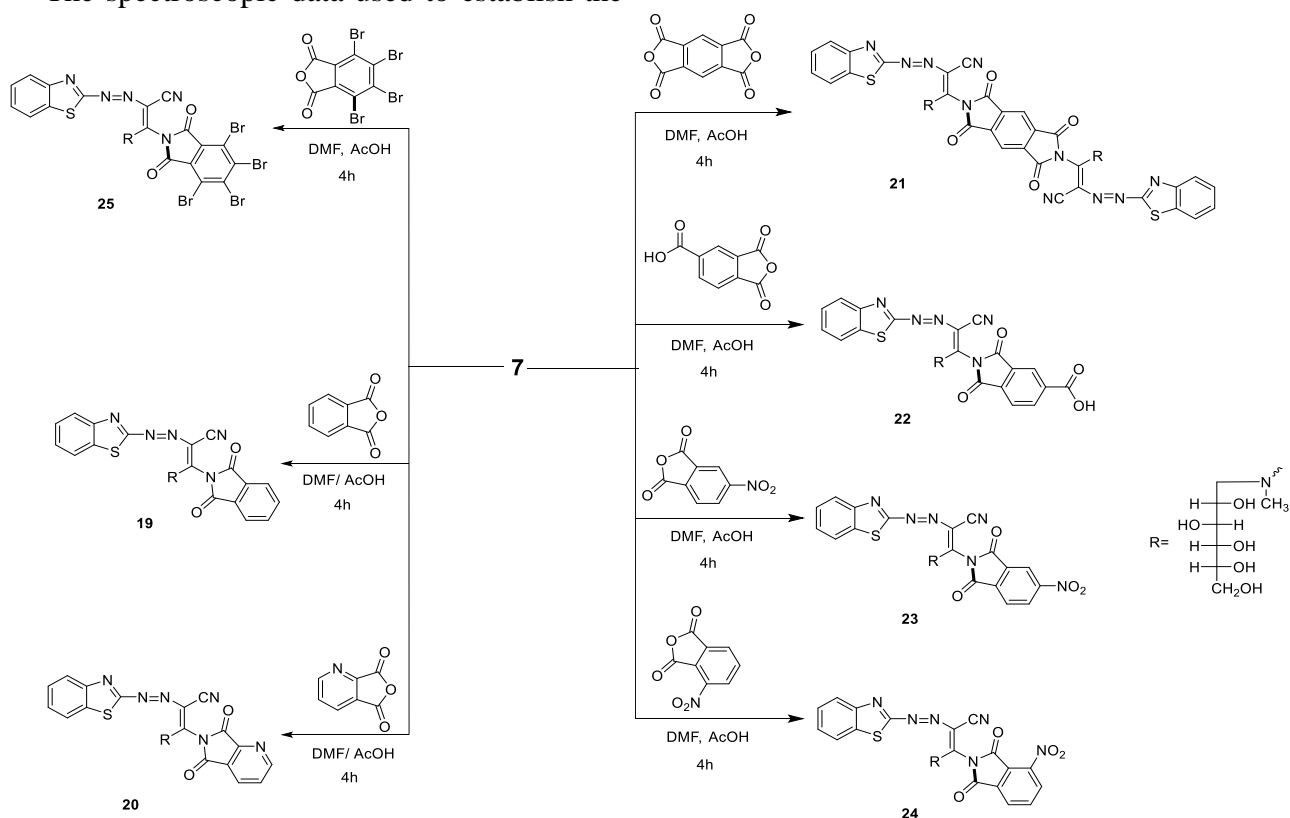


Scheme 3

When compound **7** was refluxed with various acid anhydrides such as phthalic anhydride, quinolinic anhydride, pyromellitic anhydride, 1,2,4-benzene tricarboxylic anhydride, 4-nitrophthalic anhydride, 3-nitrophthalic anhydride, and/or tetrabromophthalic anhydride, the resulting phthalimide derivatives **19–25** were obtained, respectively (**Scheme 4**).

The spectroscopic data used to establish the

structures of compounds **19–25** showed that the NH_2 group vanished from their IR spectra and displayed an absorption band at $\approx 1700\text{--}1680\text{ cm}^{-1}$ that was attributable to the amidic carbonyl function. Additionally, molecular ion peaks at m/z (%) = 552 (M^+ , 40), 553 (M^+ , 48), 596 (M^+ , 44), 597 (M^++1 , 48), and 868 (60), respectively, were obtained in the mass analyses of compounds **19**, **20**, **22**, and **25**.

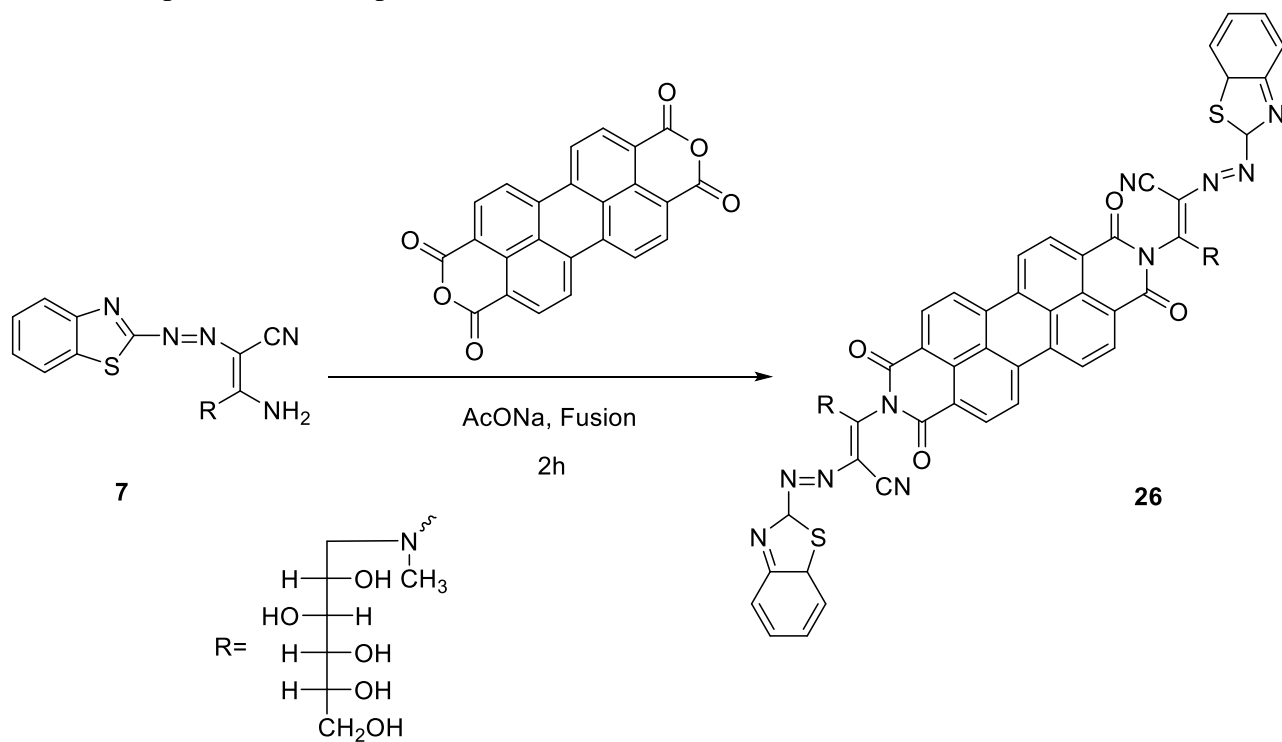


Scheme 4

Compound **26** was obtained by fusing the enaminonitrile derivative **7** with the 3,4,9,10-perylenetetracarboxylic dianhydride in the presence of freshly fused sodium acetate (Scheme 5).

The IR spectrum of compound **26** revealed

absorption bands at 3455-3445, 2200, 2220, 1710-1685, and 1535, 1515 cm^{-1} , respectively, corresponding to OH, CN, CO, and N=N groups. This confirmed the structure of compound **26**.

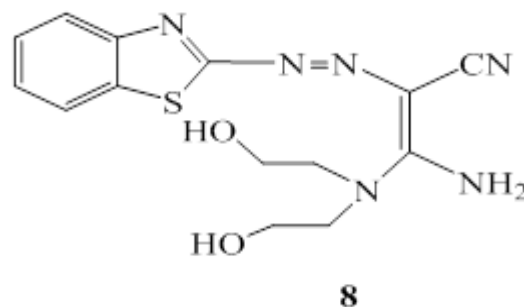
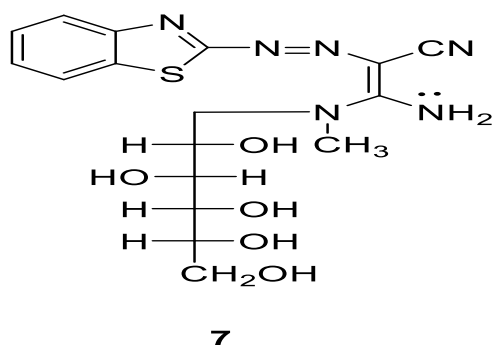


Scheme 5

2.2. Pharmacological Evaluation Antioxidant activity ABTS

According to previous studies, the antioxidant activity assay was performed [34].

The ability of each substance to reduce the rate of erythrocyte hemolysis they were evaluated for their antioxidant activity by their capacity to reduce lipid peroxidation in rat brain and kidney homogenates. Using the ABTS test, the compounds' pro-oxidant activities were evaluated for their antioxidant properties. In the current study, **Table 1** displayed the novel compounds' antioxidant results.



The ABTS radical cation was only somewhat inhibited by compounds **9** and **11**, which don't include any glucaminoid moiety.

Compound **26** is distinguished by the presence of two glucaminoid moieties; however, it has only moderate activity (58.04%), which may be due to its large size, which makes it difficult to penetrate the cell.

It was found that compounds **7** and **8** have strong antioxidative action. Compounds **19**, **22**, **23**, and **24** demonstrated excellent action in contrast. In terms of erythrocyte hemolysis, compounds **7**, **8**, and **19–24** displayed strong

activity, while compounds **14**, **15**, **16**, **17**, **20**, and **25** exhibited moderate activity most of the time.

By comparing the tested compounds, we can conclude the following structure-activity relationships (SARs) from **Table 1** and the above-mentioned results:

1- The presence of glucamenoid and ethanol amine moieties enhanced the activity.

2- Introducing phthalimide moiety enhanced also the activity.

3- The presence of pyrimidine (compound **14**) and pyridine (compound **16**) did not affect the antioxidant activity.

AAPH-induced RBC hemolysis

According to the reported work [34], hemolysis was determined.

Bleomycin-dependent DNA damage

A family of anticancer antibiotics known as

Table 1: ABTS (free radical scavenging) and erythrocyte hemolysis of the new benzothiazole compounds

Comp No.	ABTS (% ofscavenging Inhibition)a,b,c,d,e	Erythrocyte hemolysis(%)
Ascorbic acid	80.81 ± 1.16	0.85
3	47.77 ± 2.50	1.95
4	45.72 ± 2.38	1.90
7	79.79 ± 1.34	0.86
8	76.06 ± 0.23	0.84
9	48.45 ± 1.15	1.90
11	45.50 ± 0.16	1.01
14	60.91 ± 1.30	1.01
15	57.54 ± 0.24	1.91
16	63.50 ± 1.35	1.83
17	55.58 ± 0.25	1.01
18	50.58 ± 1.30	1.91
19	73.04 ± 1.24	0.84
20	68.04 ± 0.14	0.96
21	60.91 ± 0.04	0.91
22	74.64 ± 0.32	0.86
23	75.26 ± 0.29	0.84
24	72.45 ± 0.12	0.91
25	65.79 ± 1.32	0.80
26	58.04 ± 1.74	1.85

ABST Scavenging activity (%) is computed as $[Ac - As / Ac] \times 100$, where "Ac" is the absorbance value of the control and "As" is the absorbance of the additional samples test solution.

Table 2: Bleomycin-dependent DNA damage assays of the isolated benzothiazole compounds.

Comp No.	Absorbance
Ascorbic acid	0.00881
7	0.00858
8	0.00882

bleomycin is frequently employed as an antitumor medication. It has been decided to use the bleomycin assay to evaluate the pro-oxidant impact of dietary antioxidants. Bleomycin, an anticancer antibiotic, binds iron ions and DNA. When heated with thiobarbituric acid, DNA that has been degraded by the bleomycin iron complex produces a pink chromogen. Antioxidants that are added to a reducing agent compete with DNA and reduce chromogen production. We analyze the bleomycin-dependent DNA damage caused by ABTS, erythrocyte hemolysis, and the top antioxidant activity outcomes.

It was assessed considering previously published work [34]. According to **Table 2**, compounds **7** and **8** have the best anti-damage activity against DNA, which reduces the production of chromogen when thiobarbituric acid (TBA) comes into contact with damaged DNA.

Antitumor testing

The ability of newly synthesized compounds **3**, **4**, **7**, **8**, **9**, **11**, **14-18**, and **19-26** to inhibit tumor growth in four different cell lines; the human hepatocellular liver carcinoma (**HepG2**), the human lung fibroblast (**WI-38**), the African green monkey kidney epithelial cells (**VERO**), and the human breast

adenocarcinoma (MCF-7) cell lines was evaluated [35].

The cytotoxicity was determined by determining IC₅₀ that caused a 50% loss of cell monolayer (Table 3).

Compounds 7, 8, 9, 11 and 14 have significantly higher ABTS and anticancer activity than the other compounds, according to Tables 1 and 3. According to this investigation, the majority of the synthesized compounds 7, 8, 9, 11, 14, 19–25 are effective against the HepG2 cell line. Compounds 7, 8, 9, 11, and 14 were also found to be potent against the WI-38 cell line. Additionally, compounds 7, 11, 20, and 21 were found to be effective against VERO cell lines. Contrarily, compounds 14, 15, 16, and 21 are effective against the MCF-7 cancer cell.

Structure-activity relationship:

It is commonly known that the fundamental units of DNA's structure are nucleotide moieties. Cytosine (C), guanine (G), thymine (T), and adenine (A) are just a few of the several nitrogen bases that can be found in the structure of a nucleotide. A hydrogen bond normally holds adenine and cytosine together.

Two factors [36, 37] influence the cytotoxic action against tumor cell lines:

(1) The appearance of an intramolecular hydrogen bond with bases of DNA.

(2) The investigated compounds electrostatic attraction to the cell wall.

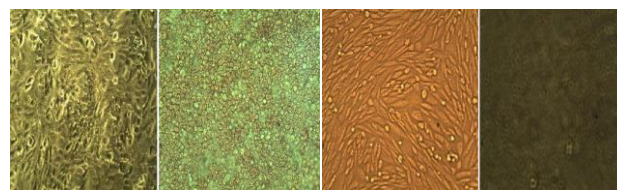
After a report on the cytotoxicity of the compounds under investigation and their structure-activity relationship:

1- One of the DNA nucleobases and Intermolecular hydrogen bonding between NH and NH₂ groups, which may cause damage to DNA, may explain why compounds 9 and 11 all display high activity.

2- In addition, although compounds 19–26 include two amidic carbonyl groups, which both function as potent electron-drawing groups that engage electrostatically with DNA nucleobases, compounds 15–17 have ester groups.

3- All of the synthesized compounds which have an NH group, can form a harmful intermolecular hydrogen bond with DNA nucleobases.

4- Pyrazine 9 has significant cytotoxic action and damages DNA due to the hydrogen bond it forms with DNA nucleobases.



Vero Cells WI 38 HepG2 MCF-7

Table 3: The antitumor activity of examined benzothiazole compounds on various cancer cells.

CompNo.	"IC ₅₀ , (µg/mL)" *			
	"HepG-2"	"WI-38"	"VERO"	"MCF-7"
3	62 ± 0.08	86 ± 0.12	74 ± 0.22	58 ± 1.30
4	60 ± 0.08	84 ± 0.12	72 ± 0.22	50 ± 1.30
7	15 ± 0.14	19 ± 0.13	22 ± 0.23	35 ± 0.06
8	18 ± 0.12	21 ± 0.25	31 ± 0.15	41 ± 1.24
9	16 ± 0.05	17 ± 1.02	42 ± 1.02	40 ± 1.34
11	14 ± 0.13	17 ± 0.29	25 ± 0.12	32 ± 0.45
14	11 ± 0.12	15 ± 1.32	41 ± 0.11	22 ± 0.23
15	48 ± 0.05	70 ± 0.12	109 ± 0.09	20 ± 0.01
16	42 ± 0.25	60 ± 0.25	111 ± 0.02	25 ± 0.22
17	44 ± 1.24	39 ± 0.05	40 ± 0.05	32 ± 0.38
18	22 ± 0.22	39 ± 0.17	54 ± 0.22	34 ± 2.01
19	16 ± 0.01	40 ± 0.14	36 ± 0.15	43 ± 0.12
20	12 ± 0.48	27 ± 0.34	25 ± 0.23	43 ± 0.06
21	21 ± 3.02	22 ± 0.23	20 ± 0.36	18 ± 1.02
22	17 ± 1.35	89 ± 0.05	37 ± 0.04	26 ± 0.01
23	19 ± 0.15	37 ± 0.07	38 ± 0.02	27 ± 0.05
24	19 ± 0.29	42 ± 0.01	41 ± 0.01	40 ± 0.13
25	21 ± 0.18	24 ± 0.03	36 ± 0.05	52 ± 0.05
26	51 ± 0.02	89 ± 0.01	65 ± 0.05	37 ± 0.12
5-Fu	8.6 ± 0.04	3.2 ± 0.11	6.5 ± 0.03	2.3 ± 0.01

2.3. Molecular docking

Solid tumor growth and progression are significantly influenced by the epidermal growth factor receptor (EGFR).

There is mounting evidence that EGFR activation also plays a role in the resistance to radiation and chemotherapy.

Studies clarifying the biochemical basis of these observations have shown that EGFR inhibition down-regulates the survival pathways dependent on PI3-K/Akt or mitogen-activated protein kinase (MAPK) or PI3-K/Akt in many tumor types and is linked to a proapoptotic shift in Bcl-2 expression and/or activation [38].

The binding disposition of the docked compounds, in particular **7**, **8**, and **11**, **14**, towards the binding site of EGFR complexed with co-crystallized ligand, was investigated using molecular docking (PDB=1M17).

As can be observed in **Table 4**, all of the compounds formed the same binding interactions with the amino acids met 769 when docked with binding energies ranging from -16.64 to -22.08 Kcal/mol.

It's interesting to note that compound **14** preserved the co-crystallized ligand's binding disposition and successfully developed an interaction binding mode with the important amino acid Met 769, as shown in **Figure 3**.

Because of this, docking experiments showed that the EGFR protein was bound virtually by docked molecules.

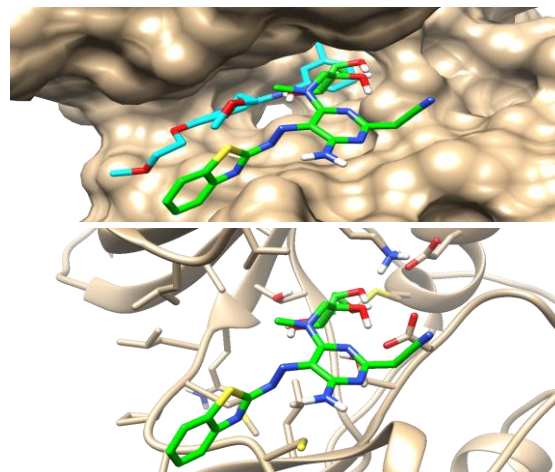
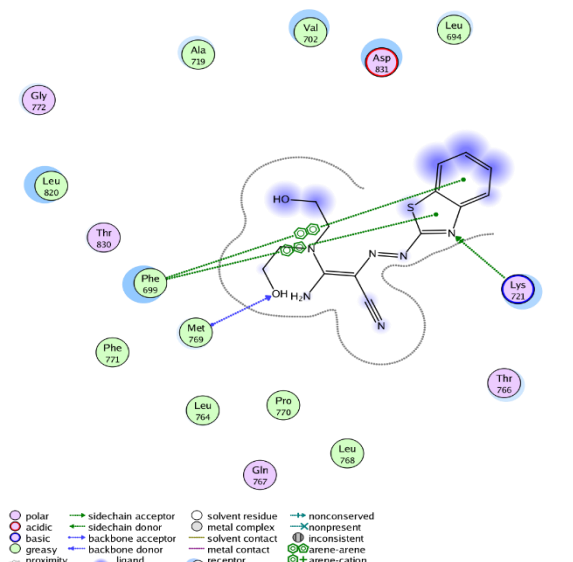
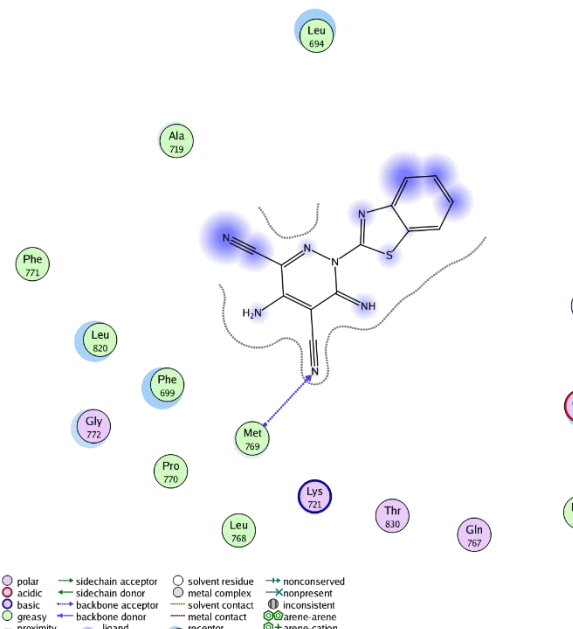
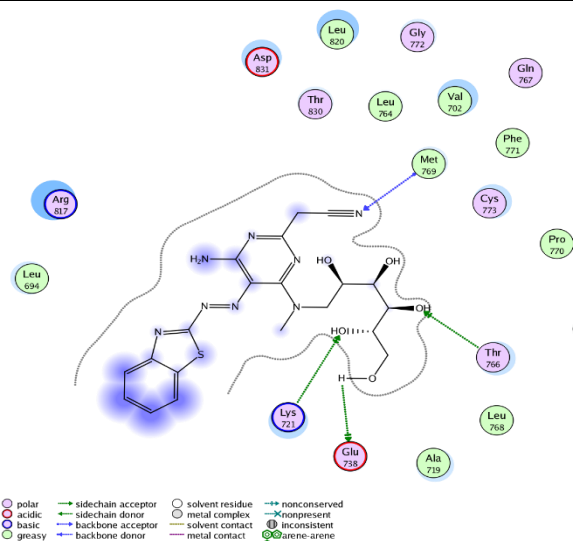


Figure 3: Binding disposition of the docked compound **14** inside the EGFR protein. **A:** Surface view and **B:** Interactive view

Table 4: Ligand-receptor interactions of the docked compounds **7**, **8**, **11**, and **14** with binding energies (Kcal/mol) inside the Bcl-2 protein (PDB=4LVT) using MOE software*

Compound	Docking score (Kcal/mol)	2D Interactive pose	Ligand-receptor interactions with key amino acids
7	-21.31		1 1 H-bond with Met 769

8	-17.62		1 H-bond with Met 769
11	-12.64		1 H-bond with Met 769
14	-22.08		1 H-bond with Met 769

* Docking calculation using MOE software was validated by having a good binding disposition with the co-crystallized ligand (RMSD lower than 2.5).

3. Experiment

3.1. Material and Methods

N-(benzo[d]thiazol-2-yl)carbon-hydrazoneoyl dicyanide (**2**) was prepared by the reported literature [39]

Synthesis of compounds (3-8)

General procedure:

They were obtained from previously reported literature [40].

(2Z)-3-amino-2-(benzo[d]thiazol-2-yl)diazenyl-3-(piperidin-1-yl)acrylonitrile (**3**)

Yield (0.82 g, 66%); mp 157 °C. Anal. for C₁₅H₁₆N₆S (312.40): Calculated.: C, 57.67; H, 5.16; N, 26.90%. Found: C, 57.55; H, 5.10; N, 26.81%.

(2Z)-3-amino-2-(benzo[d]thiazol-2-yl)diazenyl-3-morpholinoacrylonitrile (**4**)

Yield (1.20 g, 74%); mp 142 °C. Anal. for C₁₄H₁₄N₆OS (314.37): Calcd.: C, 53.49; H, 4.49; N, 26.73%. Found: C, 53.37; H, 4.41; N, 26.66%.

(2Z)-3-amino-2-(benzo[d]thiazol-2-yl)diazenyl-3-(piperazin-1-yl)acrylonitrile (**5**)

Yield (0.66 g, 64%); m.p. 163 °C. Anal. for C₁₄H₁₅N₇S (313.38): Calculated: C, 53.66; H, 4.82; N, 31

(2Z)-3-amino-2-(benzo[d]thiazol-2-yl)diazenyl-3-(diphenylamino)acrylonitrile (**6**)

Yield (0.73 g, 71%); mp 181 °C. Anal. for C₂₂H₁₆N₆S (396.47): Calculated: C, 66.65; H, 4.07; N, 21.20%. Found: C, 66.57; H, 3.98; N, 21.12%.

(2Z)-3-amino-2-(benzo[d]thiazol-2-yl)diazenyl-3-(methyl((2S,3R,4R,5R)-2,3,4,5,6-pentahydroxyhexyl)amino)acrylonitrile (**7**)

Yield (0.68 g, 72%); mp 196 °C. Anal. for C₁₇H₂₂N₆O₅S (422.46): Calculated: C, 48.33; H, 5.25; N, 19.89%. Found: C, 48.27; H, 5.20; N, 19.77%.

(2Z)-3-amino-2-(benzo[d]thiazol-2-yl)diazenyl-3-(bis(2-hydroxyethyl)amino)acrylonitrile (**8**)

Yield (0.56 g, 58%); mp 166 °C. Anal. for C₁₄H₁₆N₆O₂S (332.38): Calculated: C, 50.59;

H, 4.85; N, 25.28%. Found: C, 50.51; H, 4.78; N, 25.21%.

Synthesis of 4-(benzo[d]thiazol-2-yl)diazenyl-1H-pyrazole-3,5-diamine (**9**) [40].

Orange powder; yield (0.76 g, 76%); mp 156 °C. Anal. for C₁₀H₉N₇S (259.29): Calculated: C, 46.32; H, 3.50; N, 37.81%. Found: C, 46.22; H, 3.39; N, 37.77%.

Synthesis of 4-amino-1-(benzo[d]thiazol-2-yl)-6-imino-1,6-dihydropyridazine-3,5-dicarbonitrile (**11**) [40].

Brown powder; yield (0.68 g, 71%); mp 166 °C. Anal. for C₁₃H₇N₇S (293.31): Calculated C, 53.24; H, 2.41; N, 33.43%. Found: C, 53.18; H, 2.33; N, 33.39%.

Synthesis of 2-(4-amino-5-(benzo[d]thiazol-2-yl)diazenyl)-6-(methyl((2S,3R,4R,5R)-2,3,4,5,6-pentahydroxyhexyl)amino)pyrimidin-2-yl)acetoneitrile (**14**) [40].

Orange crystals; yield (0.62 g, 68%); mp 186 °C. Anal. for C₂₀H₂₄N₈O₅S (488.52): Calculated: C, 49.17; H, 4.95; N, 22.94%. Found: C, 49.15; H, 4.88; N, 22.86%.

Synthesis of (2R,3R,4R,5S)-6-(((1E)-1-(N-acetylacetamido)-2-(benzo[d]thiazol-2-yl)diazenyl)-2-cyanovinyl(methyl)amino)-hexane-1,2,3,4,5-pentayl pentaacetate (**15**) [40].

Brown powder; yield (0.66 g, 70%); mp 123 °C. Anal. for C₃₁H₃₆N₆O₁₂S (716.72): Calculated: C, 51.95; H, 5.06; N, 11.73%. Found: C, 51.82; H, 4.99; N, 11.69%.

Synthesis of (2R,3R,4R,5S)-6-((1-acetyl-4-amino-3-(benzo[d]thiazol-2-yl)diazenyl)-6-oxo-1,6-dihydropyridin-2-yl(methyl)amino)hexane-1,2,3,4,5-pentayl pentaacetate (**16**) [40].

Black crystals; yield (0.63 g, 68%); mp 147 °C. Anal. for C₃₁H₃₆N₆O₁₂S (716.72): Calculated: C, 51.95; H, 5.06; N, 11.73%. Found: C, 51.88; H, 5.00; N, 11.66%.

Synthesis of (2R,3R,4R,5S)-6-(((1E)-2-(benzo[d]thiazol-2-yl)diazenyl)-2-cyano-1-((E)-ethoxymethylene)amino)vinyl(methyl)amino)hexane-1,2,3,4,5-pentayl pentaacetate (**17**)

It was formed according to previously reported work [40].

Brown crystals; yield (0.61 g, 65%); mp 133 °C. Anal. for C₃₀H₃₆N₆O₁₁S (688.71): Calculated: C, 52.32; H, 5.27; N, 12.20%. Found: C, 52.27; H, 5.21; N, 12.16%.

Synthesis of (1E)-N'-((1E)-2-(benzo[d]thiazol-2-yl diazenyl)-2-cyano-1-(methyl((2S,3R,4R,5R)-2,3,4,5,6-pentahydroxyhexyl)amino)vinyl)-N,N-dimethylformimidamide (18) [40].

Brown crystals; yield (0.73 g, 78%); mp 176 °C. Anal. for C₂₀H₂₇N₇O₅S (477.54): Calculated: C, 50.30; H, 5.70; N, 20.53%. Found: C, 50.26; H, 5.63; N, 20.44%.

Reaction of compound 7 with anhydrides [40].

Compound (19); brown powder; yield (0.66 g, 70%); mp 175 °C. Anal. for C₂₅H₂₄N₆O₇S (552.56): Calculated: C, 54.34; H, 4.38; N, 15.21%. Found: C, 54.22; H, 4.22; N, 15.18%.

Compound (20); brown crystals; yield (0.58 g, 64%); mp 185 °C. Anal. for C₂₄H₂₃N₇O₇S (553.55): Calculated: C, 52.08; H, 4.19; N, 17.71%. Found: C, 51.98; H, 4.15; N, 17.66%.

Compound (21); brown powder; yield (0.47 g, 54%); mp over 300 °C. Anal. for C₄₄H₄₂N₁₂O₁₄S₂ (1027.01): Calculated: C,

51.46; H, 4.12; N, 16.37%. Found: C, 51.37; H, 4.08; N, 16.28%.

Compound (22); brown powder; yield (0.42 g, 61%); mp 188 °C. Anal. for C₂₆H₂₄N₆O₉S (596.57): Calculated: C, 52.35; H, 4.06; N, 14.09%. Found: C, 52.22; H, 3.88; N, 13.92%.

Compound (23); brown powder; yield (0.48 g, 52%); mp 210 °C. Anal. for C₂₅H₂₃N₇O₉S (597.56): Calculated: C, 50.25; H, 3.88; N, 16.41%. Found: C, 50.18; H, 3.69; N, 16.37%.

Compound (24); brown powder; yield (0.37 g, 44%); mp 180 °C. Anal. for C₂₅H₂₃N₇O₉S (597.56): Calculated: C, 50.25; H, 3.88; N, 16.41%. Found: C, 50.18; H, 3.69; N, 16.37%.

Compound (25); black powder; yield (0.30 g, 68%); mp over 300 °C. Anal. for C₂₅H₂₀Br₄N₆O₇S (868.15): Calculated C, 34.59; H, 2.32; N, 9.68%. Found: C, 34.48; H, 2.22; N, 9.65%.

The reaction of compound 7 with 3,4,9,10-perylenetetracarboxylic dianhydride [40].

Compound (26); black powder; yield (0.37 g, 48%); mp over 300 °C. Anal. for C₅₈H₅₂N₁₂O₁₄S₂ (1205.24): Calculated: C, 57.80; H, 4.35; N, 13.95%. Found: C, 57.77; H, 4.28; N, 13.88%.

Table 5: IR, ¹H-NMR, ¹³C-NMR, and MS of the prepared benzothiazole compounds:

Comp No.	IR(v/cm ⁻¹)	¹ H-NMR(DMSO- <i>d</i> ₆) (ppm)	¹³ C-NMR "100 MHz, DMSO- <i>d</i> ₆ " (ppm)	Mass Spectra MS (EI, 70 eV)m/z (%)
3	3450, 3350 (NH ₂), 2180 (C≡N)	1.55-1.70 (m, 2H), 1.72-1.85 (m, 4H), 3.06 (t, 4H), 6.51 (s, 2H), 7.29 (d, 2H), 7.60 (d, 2H).	24.6, 26.0 (2C), 52.8 (2C), 87.5, 114.5, 121.6, 121.8, 124.6, 125.4, 136.3, 148.7, 165.9, 173.5.	313 (M ⁺ +1, 16), 312 (M ⁺ , 30), 197 (11), 169 (15), 163 (76), 150 (10), 120 (45), 105 (78), 84 (35), 77 (100).
4	3455, 3350 (NH ₂), 2185, (C≡N)	3.14 (t, 4H), 3.67 (t, 4H), 6.54 (s, 2H), 7.42 (d, 2H), 7.75 (d, 2H).	51.5 (2C), 66.8 (2C), 87.5, 114.2, 121.6, 121.8, 124.5, 125.3, 136.3, 148.7, 165.9, 173.5.	315 (M ⁺ +1, 15), 314 (M ⁺ , 25), 197 (11), 169 (15), 163 (76), 150 (10), 120 (45), 105 (78), 84 (35), 77 (100).
5	3453, 3354 (NH ₂), 3145 (NH), 2182 (C≡N)	1.09 (s, 1H), 3.16 (t, 4H), 3.69 (t, 4H), 6.54 (s, 2H), 7.32 (d, 2H), 7.60 (d, 2H).	47.7 (2C), 52.6 (2C), 87.5, 114.2, 121.6, 121.8, 124.5, 125.3, 136.3, 148.7, 165.9, 173.5.	314 (M ⁺ +1, 15), 313 (M ⁺ , 31), 292 (48), 268 (37), 249 (37), 216 (34), 203 (32), 188 (33), 169 (55), 165 (40), 147 (46), 135 (37), 117 (37), 92 (57), 77 (100).
6	3455, 3356 (NH ₂), 2182, (C≡N), 1520 (N=N)	-----	89.5, 114.7, 121.6, 121.8, 121.9 (2C), 124.5, 125.6, 127.0 (4C), 129.6 (4C), 136.6, 141.9 (2C), 148.7, 165.9 (2C).	397 (M ⁺ +1, 23), 396 (M ⁺ , 30), 368 (12), 357 (20), 320 (14), 292 (12), 274 (8), 215 (21), 187 (28), 169 (11), 144 (9), 117 (15), 105 (16), 91 (37), 77 (100).
7	3455-3443 (OH), 3375, 3350 (NH ₂), 2954 (C-H), 2180 (C≡N),	3.04 (s, 3H), 3.56-3.62 (m, 8H), 3.93 (s, 1H), 4.35-4.51 (m, 4H), 6.45 (s, 2H), 7.25 (d, 2H), 7.53 (d, 2H).	50.7, 54.1, 64.4, 70.5, 72.0, 72.5 (2C), 87.5, 114.6, 121.6, 121.8, 124.5, 125.3, 136.3, 148.7, 165.9, 173.5.	423 (M ⁺ +1, 18), 422 (M ⁺ , 48), 370 (69), 350 (63), 331 (68), 305 (63), 289 (69), 268 (68), 258 (77), 245 (86), 234 (69), 216 (77), 203 (68), 189 (80), 174 (85), 158

	1555 (N=N)			(100), 144 (77), 136 (76), 112 (71), 109 (82).
8	3415-3455 (OH), 3450-3360 (NH ₂), 2180, (C≡N), 1535 (N=N).	3.16 (t, 4H), 3.87 (t, 4H), 4.85 (s, 2H), 6.50 (s, 2H), 7.40 (d, 2H), 7.70 (d, 2H).	53.1 (2C), 59.4 (2C), 87.5, 114.6, 121.6, 121.8, 124.5, 125.3, 136.3, 148.7, 165.9, 173.5.	333 (M ⁺ +1, 15), 332 (M ⁺ , 38), 272 (20), 197 (17), 167 (23), 120 (25), 105 (15), 92 (59), 77 (100).
9	3414-3350 (2NH ₂), 3190 (NH), 1530 (N=N).	6.20 (s, 4H), 7.41 (d, 2H), 7.70 (d, 2H), 12.53 (s, 1H).	74.4, 121.6, 121.8, 124.6, 125.1, 136.3, 148.7, 151.3, 165.9.	260 (M ⁺ +1, 10), 259 (M ⁺ , 29), 219 (5), 185 (5), 173 (5), 153 (5), 129 (5), 125 (71), 105 (15), 91 (14), 77 (100).
11	3450, 3336 (NH ₂), 3214 (NH), 2200, 2180 (2C≡N).	4.80 (s, 2H), 7.40 (d, 2H), 7.70 (d, 2H), 9.40 (s, 1H).	81.2, 115.1, 115.8, 118.3, 121.8, 124.5, 125.3, 130.8, 153.2, 154.4, 155.0, 162.7, 174.5.	294 (M ⁺ +1, 15), 293 (M ⁺ , 48), 292 (5), 276 (24), 244 (5), 216 (9), 197 (19), 187 (14), 169 (15), 142 (5), 117 (5), 105 (25), 91 (30), 77 (100).
14	3457-3382 (OH), 3350, 3340 (NH ₂), 3150 (NH), 2209 (C≡N).	3.04 (s, 3H), 3.56-3.62 (m, 8H), 3.82 (s, 2H), 3.93 (s, 1H), 4.35-4.54 (m, 4H), 7.25 (d, 2H), 7.53 (d, 2H), 8.45 (s, 2H).	23.8, 36.1, 62.7, 64.4, 69.9, 70.5, 72.5, 72.6, 79.5, 117.8, 121.6, 121.8, 124.5, 125.3, 136.3, 148.7, 159.4, 160.3, 165.4, 165.9.	489 (M ⁺ +1, 21), 488 (M ⁺ , 40), 459 (9), 446 (17), 424 (17), 407 (15), 197 (18), 120 (28), 105 (13), 84 (100), 77 (59).
15	2960 (C-H), 2174 (C≡N), 1730-1705 (5C=O), 1680 (2C=O).	2.03 (m, 15H), 2.29 (s, 6H), 3.39 (s, 3H), 3.55-3.76 (m, 2H), 4.20-4.42 (m, 2H), 5.20-5.85 (m, 4H), 7.33 (d, 2H), 7.65 (d, 2H).	15.0, 20.7, 21.0 (5C), 37.0, 31.2, 61.6, 63.8, 67.4, 68.7, 69.0, 70.8, 106.2, 114.6, 121.6, 121.8, 124.5, 125.3, 136.3, 148.7, 155.7, 165.9, 170.2 (4C), 172.5 (2C).	717 (M ⁺ +1, 33), 716 (M ⁺ , 46), 553 (51), 524 (63), 449 (33), 421 (28), 404 (61), 389 (15), 359 (48), 210 (33), 134 (48), 92 (78), 77 (86).
16	3380, 3350 (NH ₂), 1730-1705 (5C=O), 1680 (2C=O).	-----	15.0, 20.7, 21.0 (5C), 37.0, 31.2, 61.6, 63.8, 67.4, 68.7, 69.0, 70.8, 106.2, 114.6, 121.6, 121.8, 124.5, 125.3, 136.3, 148.7, 155.7, 165.9, 170.2 (5C), 172.5.	717 (M ⁺ +1, 33), 716 (M ⁺ , 46), 553 (51), 525 (63), 449 (33), 421 (28), 404 (61), 389 (15), 359 (48), 210 (33), 133 (48), 92 (78), 77 (86).
17	2179 (C≡N), 1730-1710 (5C=O), 1543, 1680 (C=O).	1.24 (t, 3H), 2.02 (m, 15H), 3.45 (s, 3H), 3.65 (q, 2H), 3.85-4.05 (m, 2H), 4.30-4.50 (m, 2H), 5.20, 5.85 (m, 4H), 7.30 (d, 2H), 7.64 (d, 2H), 8.50 (s, 1H).	15.0, 20.7, 21.0 (4C), 37.0, 31.2, 61.6, 63.8, 67.4, 68.7, 69.0, 70.8, 106.2, 114.6, 121.6, 121.8, 124.5, 125.3, 136.3, 148.7, 155.7, 165.9, 170.2 (5C), 172.5.	689 (M ⁺ +1, 32), 688 (M ⁺ , 44), 526 (51), 525 (68), 506 (62), 490 (66), 480 (76), 464 (64), 453 (66), 445 (82), 433 (73), 414 (89), 393 (82), 376 (64), 357 (66), 338 (84), 332 (74), 314 (66), 298 (76), 274 (62), 258 (68), 239 (71), 229 (68), 214 (76), 203 (100), 183 (92), 152 (69), 134 (91), 116 (71), 111 (83), 97 (77).
18	3455-3443 (OH), 2177 (C≡N), 1616 (C=N), 1550 (N=N).	2.90 (s, 6H), 3.04 (s, 3H), 3.45 (d, 2H), 3.65 (m, 6H), 3.93 (s, 1H), 4.35-4.51 (m, 4H), 7.25 (d, 2H), 7.53 (d, 2H), 8.73 (s, 1H).	36.0, 37.0, 54.5, 64.5, 70.5, 72.0, 73.0 (2C), 106.0, 114.5, 120.0 (2C), 123.0 (2C), 126.0 (2C), 129.0 (2C), 131.0, 149.0, 150.0, 153.0, 155.0, 166.2, 173.0.	478 (M ⁺ +1, 21), 477 (M ⁺ , 38), 456 (55), 437 (20), 427 (15), 405 (15), 391 (15), 371 (6), 346 (15), 323 (5), 312 (6), 285 (21), 279 (5), 161 (15), 137 (15), 85 (55), 71 (60).
19	3455-3440 (OH), 2192 (C≡N), 1690, 1680 (2C=O, amide).	-----	-----	553 (M ⁺ +1, 26), 552 (M ⁺ , 40), 512 (25), 500 (25), 480 (25), 470 (30), 452 (100), 434 (55), 419 (20), 196 (20), 120 (10), 105 (20), 93 (45), 77 (100), 64 (25).
20	3450-3445 (OH), 2200 (C≡N), 1690,	-----	-----	554 (M ⁺ +1, 26), 553 (M ⁺ , 48), 536 (30), 494 (60), 469 (10), 452 (20), 429 (15), 405 (25), 389 (25),

	1680 (2C=O, amide), 1530 (N=N).			377 (25), 361 (30), 341 (30), 319 (30), 306 (25), 285 (25), 276 (60), 259 (40), 196 (30), 181 (15), 167 (15), 143 (20), 128 (100), 117 (60), 101 (65), 93 (100), 77 (100), 59 (85).
21	3450-3440 (OH), 2193, 2200 (2C≡N), 1700-1680 (4C=O, amide).	-----	-----	
22	3500-3440 (OH), 2195 (C≡N), 1690, 1680, (2C=O, amide), 1730 (C=O).	-----	-----	597 (M ⁺ +1, 28), 596 (M ⁺ , 44), 563 (40), 551 (40), 535 (30), 522 (40), 514 (30), 386 (10), 371 (15), 281 (10), 266 (40), 197 (10), 167 (10), 148 (15), 120 (20), 105 (20), 93 (75), 77 (100), 64 (60).
23	3455-3440 (OH), 2210 (C≡N), 1690, 1680 (2CO, amide), 1560 (N=N), 1550, 1350 (NO ₂).	-----	-----	598 (M ⁺ +1, 27), 597 (M ⁺ , 48), 544 (25), 522 (30), 514 (40), 452 (20), 276 (15), 196 (25), 120 (15), 105 (20), 93 (60), 77 (100), 64 (25).
24	3455-3440 (OH), 2210 (C≡N), 1690, 1680 (2CO, amide), 1560 (N=N), 1550, 1350 (NO ₂).	-----	-----	598 (M ⁺ +1, 27), 597 (M ⁺ , 48), 554 (23), 522 (30), 514 (40), 452 (20), 276 (15), 196 (25), 120 (15), 105 (20), 93 (60), 77 (100), 64 (25).
25	3460-3445 (5OH), 2200 (C≡N), 1685, 1680 (2CO, amide), 1540 (N=N).	-----	-----	870 (M ⁺ +2, 60), 868 (M ⁺ , 60), 786 (60), 782 (80), 764 (60), 752 (60), 741 (50), 716 (40), 710 (60), 684 (70), 664 (70), 646 (50), 623 (65), 596 (70), 581 (70), 568 (55), 543 (70), 394 (20), 197 (10), 152 (15), 120 (10), 105 (15), 93 (100), 77 (95), 64 (55).
26	3455-3445 (10OH), 2200, 2220 (2C≡N), 1710-1685 (4CO), 1535, 1515 (2N=N).	-----	-----	

3.2. Pharmacology

Antioxidant screening assay (ABTS method)

It was completed in accordance with the earlier stated work [34].

Antioxidant activity screening assay for erythrocyte hemolysis

It was carried out in accordance with the earlier research that had been published [34].

Bleomycin-dependent DNA damage assay [34].

Antitumor activity [34].

3.3. Molecular docking

Following usual work [41], the examined compounds were docked using the MOE-2019 program to the EGFR protein (PDB= 1M17) protein structures. The protein-ligand complex was created using the RCSB Protein Data Bank's access to the X-ray structure of 1M17 with its bound inhibitor Navitoclax (PDB section 1M17). The protein and ligand structures were enhanced, and their energetic properties were favored, using MOE-2019. Molecular docking results were interpreted by binding activities in terms of binding energy

and ligand-receptor interactions. After that, Chimera was used for the visualization.

4. References

1. Haider, Kashif, Sara Rehman, Ankita Pathak, Abul K. Najmi, and Mohammad S. Yar. (2021) "Advances in 2-substituted benzothiazole scaffold-based chemotherapeutic agents." *Archiv der Pharmazie* 354, no. 12: 2100246.
2. Ahmed, Mubashshir, and Seema Kothari1 Manohar V. Lokhande (2022). "Green Synthesis, Characterization and their Biological Activities of Schiff's Bases of Certain Benzothiazole Derivatives." *International Journal of Applied Chemistry* 18, no. 1: 15-26.
3. X. J. Zheng, C. S. Li, M. Y. Cui, Z. W. Song, X. Q. Bai, C. W. Liang, T. Y. Zhang, (2020) *Bioorg. Med. Chem. Lett.* 30, 127237.
4. A. E. Ghonim, A. Ligresti, A. Rabbito, A. M. Mahmoud, V. Di Marzo, N. Osman, A. H. Abadi, (2019) , *European J. Med. Chem.* 180 , 154-170.
5. T. Singh, V. K. Srivastava, K. K. Saxena, S. L. Goel, (2006) Synthesis of New Thiazolylthiazolidinylbenzothiazoles and Thiazolylazetidinybenzothiazoles as Potential Insecticidal, Antifungal, and Antibacterial Agents, *Arch. Pharm. Chem. Life. Sci.* 339, 466-472.
6. Thomas, K. K., and R. Reshmy. (2008) "A Novel Study on Bioactive 2-Substituted Amino-5-benzothiazol-2-oyl-4-phenylthiazoles." *Asian Journal of Chemistry* 20, no. 2: 1457-1463.
7. K. R. Kumar, K. N. S. Karthik, P. R. Begum, C. M. M. P. Rao, (2017) Synthesis, characterization and biological evaluation of benzothiazole derivatives as potential antimicrobial and analgesic agents, *Asian J. Pharm. Sci.*, 7, 1.
8. B. M. Mistry, R. V. Patel, Y. S. Keum, D. H. Kim, (2015) Chrysin–benzothiazole conjugates as antioxidant and anticancer agents, *Bioorg. Med. Chem. Lett.* 25, 5560-5565.
9. K. Haider, M. R. Haider, K. Neha, M. S. Yar, (2020) Free radical scavengers: An overview on heterocyclic advances and medicinal prospects, *J. Med. Chem.* 204, 112607.
10. Neha, Kumari, Md Rafi Haider, Ankita Pathak, and M. Shahar Yar(2019). "Medicinal prospects of antioxidants: A review." *European journal of medicinal chemistry* 178: 687-704.
11. S. Murtuja, M. Shaquizzaman, M. Amir, (2018) Design, Synthesis, and Screening of Hybrid Benzothiazolyl-Oxadiazoles as Anticonvulsant Agents, *Lett. Drug Des. Discov.*, 15, 4.
12. R. Bhutani, D. Pathak, G. Kapoor, A. Husain, M. A. Iqbal, (2019) Novel hybrids of benzothiazole-1,3,4-oxadiazole-4-thiazolidinone: Synthesis, in silico ADME study, molecular docking and in vivo anti-diabetic assessment, *Bioorg. Chem.* 83, 6-19.
13. Haroun, Michelyne. (2019) "Novel hybrids of pyrazolidinedione and benzothiazole as TZD analogues. rationale design, synthesis and in vivo anti-diabetic evaluation." *Medicinal Chemistry* 15, no. 6: 624-633.
14. N. S. Rao, N. Nagesh, V. N. Lakshma, S. Sunkari, R. Tokala, G. Kiranmai, A. Kamal, (2019) Design and synthesis of DNA-intercalative naphthalimide-benzothiazole/cinnamide derivatives: cytotoxicity evaluation and topoisomerase- II α inhibition, *Med. Chem. Comm.* 10, 10(1), 8683.
15. R. Chikhale, S. Thorat, R. K. Choudhary, N. Gadewal, P. Khedekar, (2018) *Bioorg. Chem.*, 77, 84.
16. G. J. Kumar, S. N. Kumar, D. Thummuri, L. B. S. Adari, V. G. M. Naidu, K. Srinivas, V. J. Rao, (2015) Synthesis and characterization of new s-triazine bearing benzimidazole and benzothiazole derivatives as anticancer agents, *Med. Chem. Res.* 24, 3991-4001.
17. J. Ma, X. Ni, Y. Gao, K. Huang, J. Liu, Y. Wang, C. Wang, (2019) Identification and biological evaluation of novel benzothiazole derivatives bearing a pyridine-semicarbazone moiety as apoptosis inducers via activation of procaspase-3 to caspase-3, *MedChemComm*, 10(3), 465.
18. McGowan, J. C., and T. Powell (1962). "Rates of decompositions of certain AZO compounds." *Recueil des Travaux*

- Chimiques des Pays-Bas **81**, no. 12: 1061-1067.
19. S Pati. (1975) *The Chemistry of the Hydrazo and Azoxy Groups, Part 1*, John Wiley, New York.
 20. Salaheldin, Abdellatif M. (2008) "Enaminonitriles in heterocyclic synthesis: Novel synthesis of 3-aminopyrroles and pyrrolo [3, 2-d] pyrimidine derivatives." *Zeitschrift für Naturforschung B* **63**, no. **5**: 564-570.
 21. Garcia-López, M. Teresa, G. Federico, and Manfred Stud. (1978) "New routes for the synthesis of pyrrolo-[3, 2-d]-and-[2, 3-d]-pyrimidine systems starting from a common pyrrole derivative." *Journal of the Chemical Society, Perkin Transactions* **1** **5**: 483-487.
 22. A. Elkholy, F. Al-Qalaf, MH Elnagdi, (2008) Synthesis and Anti-inflammatory Evaluation of Some New Pyrazole, Pyrimidine, Pyrazolo[1,5-a]Pyrimidine, Imidazo[1,2-b]Pyrazole and Pyrazolo[5,1-b]Quinazoline Derivatives Containing Indane Moiety, *Arkivocxiv* **124**–131. 420.
 23. AM. Salaheldin, (2008) AMF. Oliveira-Campos, LM. Rodrigues, 3-Aminopyrroles and their application in the synthesis of pyrrolo[3,2-d]pyrimidine (9-deazapurine) derivatives, *Arkivoc* **14** 180–190.
 24. H.M.F. Madkour, A.A.E. Afify, G.A. Elsayed, M.S. Salem. Bulg, (2008) Synthetic utility of enaminonitrile moiety in heterocyclic synthesis, *Chem. Comm.* **40** 147–159.
 25. Etson, Sandra Rae, Ronald J. Mattson, and J. Walter Sowell Sr. (1979) "Synthesis of substituted pyrrolo [2, 3-D] pyrimidine-2, 4-diones." *Journal of Heterocyclic Chemistry* **16**, no. 5: 929-933.
 26. Dyachenko VD, Dyachenko AD. (2008) Synthesis of 4-alkyl(aryl, hetaryl)-2-thioxo-5,6,7,8-tetrahydroquinoline-3-carbonitriles and their derivatives by cross-recyclization of 4-alkyl(aryl, hetaryl)-2,6-diamino-4H-thiopyran-3,5-dicarbonitriles with 4-(cyclohex-1-en-1-yl)-morpholine, alkyl halides, and cyclohexanone, *Russ. J. Org. Chem.* 412–420.
 27. Zaki MEA, Saliman HA, Hickal OA, Rashad AE. *Z. Naturforsch., C: Biosci* (2006). **61** 1–5.
 28. JL Wang, D Liu, ZJ Zhang, S Shan, X Han, SM Srinivasula, CM Croce, ES Alnemri, Z Huang. (2000) Structure-based discovery of an organic compound that binds Bcl-2 protein and induces apoptosis of tumor cells *Proc. Natl. Acad. Sci. U. S. A.* **97** 7124–7129.
 29. M. E. A. Zaki,, E. M. Morsy,, F. M. Abdel-Motti, and F. M. E. Abdel-Megeid, (2004) The Behaviour of Ethyl 1-acetyl-4-aryl-5-cyano-3-methyl-1,4-dihydropyrano[2,3-c]pyrazol-6-ylimidofomate Towards Nucleophiles, *Heterocycl. Commun.* **10** 97–102.
 30. S Bondock, R Rabie, HA Etman, AA Fadda. (2008) Synthesis and antimicrobial activity of some new heterocycles incorporating antipyrine moiety, *Eur. J. Med. Chem.* **43** 2122-2129.
 31. AA. Fadda, KhM. Elattar, (2015) Synthesis and Structure Activity Relationship of Some Indole Derivatives as Potential Anti-inflammatory Agents, *J. Biosci. Med.* **3** 114-123.
 32. El Ashry, El-SH, and Y. El Kilany. (1998) "Acyclonucleosides: Part 3. tri-, tetra-, and pentaseco-nucleosides." *Advances in heterocyclic chemistry* **69**: 129-215.
 33. Makara GM, Keseru GM. On the Conformation of Tiazofurin Analogues, *J. Med. Chem.* **40** (1997) 4154-4159.
 34. Fadda AA, Berghot MA, Amer FA, Badawy DS, Bayoumy NM. (2012) *Arch. Pharm. Chem. Life Sci (Archiv der Pharmazie)* **345** ,378–385.
 35. T. Kalai, ML Kuppasamy, M Balog, K Selvendiran, BK Rivera, P Kuppasamy, K Hideg, (2011) Synthesis of N-Substituted 3,5-Bis(arylidene)-4-piperidones with High Antitumor and Antioxidant Activity, *J. Med. Chem.* **54** 5414-5421.
 36. G. Bischoff and S. Hoffmann, (2002) DNA-Binding of Drugs Used in Medicinal Therapies, *Current Medicinal Chemistry* **9**,: 321–348.
 37. R. Martinez and L. Chacon-Garcia, (2005) The Search of DNA-Intercalators as Antitumoral Drugs: What It Worked and What Did Not Work, *Current Medicinal*

-
- Chemistry **12**, no. 2: 127–51.
38. S. Goel, M. Hidalgo, R. Perez-Soler, (2007) EGFR inhibitor-mediated apoptosis in solid tumors, *J Exp Ther Oncol.* **6** 305–320.
39. AA Fadda, AM Khalil, TAE Ameen, FA Badria, (2009) Synthesis, antitumor evaluation, molecular modeling and quantitative structure–activity relationship (QSAR) of some novel arylazopyrazolodiazine and triazine analogs, *Bioorg. & Med. Chem.* **17** 5096–5105.
40. Al-Rooqi MM, Awad RS, Obaid RJ, Jassas RS, Fadda AA, Ahmed SA. (2023) Synthesis of Pyrazole, Pyridine, and Pyrimidine Derivatives Incorporating Glucaminoid Moiety and Their Antioxidant, Antitumor Activities and Docking Study. *ChemistrySelect.* **8**, e202300972.
41. M.M. Khalifa, A.A. Al-Karmalawy, E.B. Elkaeed, M.S. Nafie, M.A. Tantawy, I.H. Eissa, H.A. Mahdy, (2022) Topo II inhibition and DNA intercalation by new phthalazine-based derivatives as potent anticancer agents: design, synthesis, anti-proliferative, docking, and in vivo studies, *Journal of Enzyme Inhibition and Medicinal Chemistry.* **37** 299–314.